A hybrid electromagnetics-circuit simulation method exploiting discontinuous Galerkin time domain finite element method

Ping Li and **Li Jun Jiang**
University of Hong Kong, Hong Kong, China e-mail: liping@eee.hku.hk

Abstract

A hybrid electromagnetics (EM)-circuit simulation method employing the discontinuous Galerkin finite element time domain method (DGFETD) is developed to model single lumped port networks comprised of both linear and non-linear elements. The whole computational domain is split into two subsystems. One is the EM subsystem that is analyzed by the DGFETD, while another is the circuit circuit subsystem that is modeled by the Modified Nodal Analysis method (MNA) to generate a circuit subsystem. The coupling between the EM and circuit subsystems is achieved through a lumped port. Due to the local properties of DGFETD operations, only small coupling matrix equation systems are involved. To solve non-linear devices, the standard Newton-Raphson method is applied to solve the established non-linear system equations. Numerical examples are presented to validate the proposed algorithm.

1 Introduction

With the ever increasing operating frequencies of microwave circuits, the minimization of chip packaging, and the requirement of multifunctional capabilities, any successful system/subsystem design must take into account unintentional emissions and couplings from lumped circuit networks. To model non-linear devices, time domain simulators are more favorable compared with frequency domain simulators since transient analysis can directly

Pulsed Electromagnetic Fields: Their Potentialities, Computation and Evaluation
I. E. Lager and L. J. Jiang (Eds.).
doi: 10.3233/978-1-61499-230-1-89

consider the non-linear properties without resorting to harmonic balance method.

Recently, many transient simulators are available to analyze the interactions between the full-wave and the circuit regions. Among them, finite-difference time-domain (FDTD) considers lumped elements by a direct stamping technique [1], using an equivalent source concept [2], or an algorithm based on the admittance matrix in Laplace domain [3].

Time domain finite element method (TDFEM) is another popular algorithm. In [4–6], TDFEM combined with the MNA is employed to study the transient behavior of non-linear devices. A global system is constructed by coupling the full-wave parts with circuit subsystems. When non-linear elements are involved, this global matrix system becomes time dependent. A significant amount of time is consumed in factorizing this matrix.

DGFETD [7] is an amenable alternative for FDTD and TDFEM. Compared with FDTD, it supports various types and shapes of elements, unstructured and non-conformal meshes. It also can achieve high order accuracy. Unlike FEM, all the operations of DGFETD are local because of its discontinuous property. In this way, the resultant mass matrix is locally coupled with the dimension equal to the number of degrees of freedom in that element. Hence, the fully explicit time marching scheme with high efficiency is obtained. In [8], DGFETD is applied to study the transient behavior of interconnect structures with linear lumped elements. The lumped elements are treated by assigning each of them onto a rectangular surface. For this kind of direct stamping method, it is quite complex or impossible to model arbitrary complex networks. In [9], the lumped network is solved by a direct recall of SPICE simulator. A lot of time is wasted on the interface communication.

The aim of this letter is to develop a hybrid EM-circuit simulator to model arbitrary complex single port networks including both linear/nonlinear elements. The EM part and circuit subsystem couples with each other through an lumped port residing over an rectangular impedance surface. The EM part is analyzed by solving the Maxwell's equation via DGFETD, while the circuit part is modeled by the MNA based on Kirchoff's circuit laws (KCL). The coupling from the EM subsystem to the circuit subsystem is achieved by introducing a voltage source at the lumped port. This voltage source is computed from the integration of the electric field obtained by DGFETD, while the coupling from the circuit subsystem to the EM subsystem is realized by introducing a current source calculated through the circuit solver at the lumped port. Compared with the FEM [4–6], the coupled system (as shown in Section 2.3) is quite small and can be solved with

trivial cost. This property is very important for circuit networks including nonlinear elements. To verify our algorithm, numerical results are presented.

2 Formulation

This section details the proposed EM-circuit simulator. The basics of DGFETD is formulated in Section 2.1, and the circuit subsystem is presented in Section 2.2. The details of the coupling scheme between the EM and circuit subsystems are described in Section 2.3.

2.1 Formulation of DGFETD

Suppose that we are concerning the electromagnetic field in the computational domain Ω bounded by $\partial\Omega$. The global domain Ω is splitted into a set of non-overlapping subdomains Ω_i bounded by a surface $\partial\Omega_i$, where $\Omega = \bigcup \Omega_i$. Applying the discontinuous Galerkin testing procedure to the two first-order Maxwell's equations leads to the following two equations,

$$\int_{\Omega_i} \boldsymbol{\Phi}_k^{(i)} \cdot \left(\epsilon \frac{\partial \boldsymbol{E}}{\partial t} - \boldsymbol{\nabla} \times \boldsymbol{H} \right) dV = \int_{\partial\Omega_i} \boldsymbol{\Phi}_k^{(i)} \cdot \left[\hat{\boldsymbol{n}} \times (\boldsymbol{H}^* - \boldsymbol{H}) - \boldsymbol{J}^{\mathrm{im}} \right] \mathrm{d}S \quad (1)$$

$$\int_{\Omega_i} \boldsymbol{\Psi}_l^{(i)} \cdot \left(\mu \frac{\partial \boldsymbol{H}}{\partial t} + \boldsymbol{\nabla} \times \boldsymbol{E} \right) \mathrm{d}V = - \int_{\partial\Omega_i} \boldsymbol{\Psi}_l^{(i)} \cdot \hat{\boldsymbol{n}} \times (\boldsymbol{E}^* - \boldsymbol{E}) \, \mathrm{d}S \quad (2)$$

where $\boldsymbol{\Phi}_k^{(i)}$ denotes the k-th vector basis function for $\boldsymbol{E}$ in the i-th subdomain and $\boldsymbol{\Psi}_l^{(i)}$ denotes the l-th vector basis function for $\boldsymbol{H}$ in i-th subdomain. $\boldsymbol{J}^{\mathrm{im}}$ represents the imposed electrical current density in the EM subsystem. Here, it is assumed to be zero. $\hat{\boldsymbol{n}}$ is the unit outward normal vector. $\hat{\boldsymbol{n}} \times \boldsymbol{H}^*$ and $\hat{\boldsymbol{n}} \times \boldsymbol{E}^*$ are called the numerical flux for communications between adjacent elements. In elements containing lumped ports, the central flux

$$\hat{\boldsymbol{n}} \times \boldsymbol{H}^* = \hat{\boldsymbol{n}} \times \frac{\boldsymbol{H}^- + \boldsymbol{H}^+}{2} - \frac{\boldsymbol{J}^{\mathrm{CKT}}}{2} \quad (3)$$

$$\hat{\boldsymbol{n}} \times \boldsymbol{E}^* = \hat{\boldsymbol{n}} \times \frac{\boldsymbol{E}^- + \boldsymbol{E}^+}{2} \quad (4)$$

is employed, which is derived from the boundary condition over the lumped ports

$$\hat{\boldsymbol{n}} \times (\boldsymbol{H}^+ - \boldsymbol{H}^-) = \boldsymbol{J}^{\mathrm{CKT}} \quad (5)$$

$$\hat{\boldsymbol{n}} \times (\boldsymbol{E}^+ - \boldsymbol{E}^-) = 0 \quad (6)$$

while the upwind flux

$$\hat{\boldsymbol{n}} \times \boldsymbol{E}^* = \hat{\boldsymbol{n}} \times \frac{(Y^- \boldsymbol{E}^- - \hat{\boldsymbol{n}} \times \boldsymbol{H}^-) + (Y^+ \boldsymbol{E}^+ + \hat{\boldsymbol{n}} \times \boldsymbol{H}^+)}{Y^- + Y^+} \tag{7}$$

$$\hat{\boldsymbol{n}} \times \boldsymbol{H}^* = \hat{\boldsymbol{n}} \times \frac{(Z^- \boldsymbol{H}^- + \hat{\boldsymbol{n}} \times \boldsymbol{E}^-) + (Z^+ \boldsymbol{H}^+ - \hat{\boldsymbol{n}} \times \boldsymbol{E}^+)}{Z^- + Z^+} \tag{8}$$

is used in the elements without lumped ports. The superscripts - and + represent local and neighboring elements, respectively. Z^- is the characteristic wave impedance in the local element and Z^+ is the characteristic wave impedance in the corresponding neighboring element. $Y^- = 1/Z^-$ and $Y^+ = 1/Z^+$ are characteristic wave admittances. $\boldsymbol{J}^{\mathrm{CKT}}$ denotes the current through the lumped port surface.

Next, the fields $\boldsymbol{E}$ and $\boldsymbol{H}$ in the domain Ω_i are expanded by local basis functions: $\boldsymbol{E} = \sum_{k=1}^{n_e^{(i)}} e_k^{(i)} \boldsymbol{\Phi}_k^{(i)}$, $\boldsymbol{H} = \sum_{l=1}^{n_h^{(i)}} h_l^{(i)} \boldsymbol{\Psi}_l^{(i)}$, where $n_e^{(i)}$ and $n_h^{(i)}$ are the number of degrees of freedom for $\boldsymbol{E}$ and $\boldsymbol{H}$ in the i-th domain, respectively. By substituting these two expressions together with (3),(4) into (1),(2), the EM matrix system in the elements where lumped ports reside can be constructed as

$$\boldsymbol{M}_e^{(i)} \frac{\partial \boldsymbol{e}^{(i)}}{\partial t} = \boldsymbol{S}_e^{(i)} \boldsymbol{h}^{(i)} - \frac{\boldsymbol{j}^{(i)}}{2} - \boldsymbol{F}_{eh}^{(ii)} \boldsymbol{h}^{(i)} + \boldsymbol{F}_{eh}^{(ij)} \boldsymbol{h}^{(j)} \tag{9}$$

$$\boldsymbol{M}_h^{(i)} \frac{\partial \boldsymbol{h}^{(i)}}{\partial t} = -\boldsymbol{S}_h^{(i)} \boldsymbol{e}^{(i)} + \boldsymbol{F}_{he}^{(ii)} \boldsymbol{e}^{(i)} - \boldsymbol{F}_{he}^{(ij)} \boldsymbol{e}^{(j)} \tag{10}$$

where

$$\left[\boldsymbol{M}_e^{(i)}\right]_{(kl)} = \int_{\Omega_i} \boldsymbol{\Phi}_k^{(i)} \cdot \epsilon \boldsymbol{\Phi}_l^{(i)} \mathrm{d}V \tag{11}$$

$$\left[\boldsymbol{M}_h^{(i)}\right]_{(kl)} = \int_{\Omega_i} \boldsymbol{\Psi}_k^{(i)} \cdot \mu \boldsymbol{\Psi}_l^{(i)} \mathrm{d}V \tag{12}$$

$$\left[\boldsymbol{S}_e^{(i)}\right]_{(kl)} = \int_{\Omega_i} \boldsymbol{\Phi}_k^{(i)} \cdot \boldsymbol{\nabla} \times \boldsymbol{\Psi}_l^{(i)} \mathrm{d}V \tag{13}$$

$$\left[\boldsymbol{S}_h^{(i)}\right]_{(kl)} = \int_{\Omega_i} \boldsymbol{\Psi}_k^{(i)} \cdot \boldsymbol{\nabla} \times \boldsymbol{\Phi}_l^{(i)} dV \tag{14}$$

$$\left(\boldsymbol{j}^{(i)}\right)_{(k)} = \int_{\partial \Omega_{i,port}} \boldsymbol{\Phi}_k^{(i)} \cdot \boldsymbol{J}^{\mathrm{CKT}} \mathrm{d}S \tag{15}$$

$$\left[\boldsymbol{F}_{eh}^{(ii)}\right]_{(kl)} = \frac{1}{2}\int_{\partial\Omega_i} \boldsymbol{\Phi}_k^{(i)} \cdot \hat{\boldsymbol{n}} \times \boldsymbol{\Psi}_l^{(i)} \mathrm{d}S \tag{16}$$

$$\left[\boldsymbol{F}_{eh}^{(ij)}\right]_{(kl)} = \frac{1}{2}\int_{\partial\Omega_i} \boldsymbol{\Phi}_k^{(i)} \cdot \hat{\boldsymbol{n}} \times \boldsymbol{\Psi}_l^{(j)} \mathrm{d}S \tag{17}$$

$$\left[\boldsymbol{F}_{he}^{(ii)}\right]_{(kl)} = \frac{1}{2}\int_{\partial\Omega_i} \boldsymbol{\Psi}_k^{(i)} \cdot \hat{\boldsymbol{n}} \times \boldsymbol{\Phi}_l^{(i)} \mathrm{d}S \tag{18}$$

$$\left[\boldsymbol{F}_{he}^{(ij)}\right]_{(kl)} = \frac{1}{2}\int_{\partial\Omega_i} \boldsymbol{\Psi}_k^{(i)} \cdot \hat{\boldsymbol{n}} \times \boldsymbol{\Phi}_l^{(j)} \mathrm{d}S \tag{19}$$

where superscript j represents the neighboring element of the i-th element. The $\boldsymbol{\Phi}_k^{(i)}$ and $\boldsymbol{\Psi}_k^{(i)}$ denote the k-th testing basis for the E and H-fields in the i-th element, respectively. The $\boldsymbol{\Phi}_l^{(j)}$ and $\boldsymbol{\Psi}_l^{(j)}$ denote the l-th basis functions for the E and H-fields in the j-th element, respectively.

The first order time derivatives will be approximated using the centering difference method, which is second order accurate. The fully discrete local system equations can be obtained from the semi-discrete system in (9) and (10) with the approximation $\boldsymbol{j}_{n+\frac{1}{2}}^{(i)} = \left(\boldsymbol{j}_{n+1}^{(i)} + \boldsymbol{j}_n^{(i)}\right)/2$ as

$$\boldsymbol{M}_e^{(i)}\boldsymbol{e}_{n+1}^{(i)} = \boldsymbol{M}_e^{(i)}\boldsymbol{e}_n^{(i)} + \Delta t\left[\left(\boldsymbol{S}_e^{(i)} - \boldsymbol{F}_{eh}^{(ii)}\right)\boldsymbol{h}_{n+\frac{1}{2}}^{(i)} \left(\boldsymbol{j}_{n+1}^{(i)} + \boldsymbol{j}_n^{(i)}\right)/4 + \boldsymbol{F}_{eh}^{(ii)}\boldsymbol{h}_{n+\frac{1}{2}}^{(j)}\right] \tag{20}$$

$$\boldsymbol{M}_h^{(i)}\boldsymbol{h}_{n+\frac{3}{2}}^{(i)} = \boldsymbol{M}_h^{(i)}\boldsymbol{h}_{n+\frac{1}{2}}^{(i)} + \Delta t\left[\left(-\boldsymbol{S}_h^{(i)} + \boldsymbol{F}_{he}^{(ii)}\right)\boldsymbol{e}_{n+1}^{(i)} - \boldsymbol{F}_{he}^{(ij)}\boldsymbol{e}_{n+1}^{(j)}\right] \tag{21}$$

2.2 Construction of circuit subsystem equations with MNA

To generate the circuit subsystem equations, the MNA based on KCL is employed to model single port lumped networks with arbitrary number of linear/non-linear elements. The resultant circuit matrix equation at time $t = (n+1)\Delta t$ is

$$\begin{bmatrix} [Y] & -[B] \\ -[B]^{\mathrm{T}} & \mathbf{0} \end{bmatrix}\begin{bmatrix} \boldsymbol{V}_{n+1}^{\mathrm{CKT}} \\ \boldsymbol{I}_{n+1}^{\mathrm{CKT}} \end{bmatrix} + \boldsymbol{I}_{n+1}^{\mathrm{CKT,nl}}\left(\boldsymbol{V}_{n+1}^{\mathrm{CKT}}\right) = \begin{bmatrix} \boldsymbol{I}_n^{\mathrm{CP}} \\ \boldsymbol{V}_{n+1}^{\mathrm{Port}} + \boldsymbol{V}_{n+1}^{\mathrm{ind}} \end{bmatrix} \tag{22}$$

where the $[Y]$ matrix is determined by interconnections between the circuit elements, the $[B]$ matrix is determined by the connection of the supplied voltage sources. $\boldsymbol{V}_{n+1}^{\mathrm{CKT}}$ denotes the unknown non-reference node voltages,

$\boldsymbol{I}_{n+1}^{\mathrm{CKT}}$ denotes the unknown currents through voltage sources. $\boldsymbol{I}_{n+1}^{\mathrm{CKT,nl}}$ represents currents through branches containing non-linear elements. $\boldsymbol{I}_{n}^{\mathrm{CP}}$ is comprised of both the supplied current source and those derived from the companion models of inductors and capacitors, $\boldsymbol{V}_{n+1}^{\mathrm{Port}}$ holds the values of the supplied voltage sources coupled from the EM part, while the $\boldsymbol{V}_{n+1}^{\mathrm{ind}}$ represents the independent voltage source in the circuit subsystem. The overall dimension of the circuit subsystem in (22), denoted as N^{CKT}, is equal to the number of non-reference voltage nodes plus the number of voltage sources.

2.3 Coupling between the EM and circuit subsystems

The coupling between the EM and circuit subsystems is achieved by introducing impressed current and voltage sources at the rectangular lumped ports with width w and length l. Since the lumped port is small compared to the wavelength, quasi-static approximation is assumed at the lumped port. It means that the electric and magnetic fields are constant over the lumped port. At the time $t = n\Delta t$, the supplied voltage at the q-th lumped port associated to i-th element is determined by DGFETD and expressed as

$$\boldsymbol{V}_{n,q}^{\mathrm{Port}} = \sum_{p=1}^{n_e} e_{n,p}^{(i)} \int \boldsymbol{\Phi}_p^{(i)} \cdot \hat{\boldsymbol{l}}_q dl = l \sum_{p=1}^{n_e} e_{n,p}^{(i)} \boldsymbol{\Phi}_p^{(i)} \cdot \hat{\boldsymbol{l}}_q = [C]_q^{(i)} \{e\}_n^{(i)} \tag{23}$$

where $\hat{\boldsymbol{l}}_q$ is the unit vector along the direction of potential descending at the q-th port. Since the current unknowns in the circuit subsystem are $\boldsymbol{I}^{\mathrm{CKT}}$ instead of $\boldsymbol{J}^{\mathrm{CKT}}$, (15) is rewritten for uniform as

$$\left(\boldsymbol{j}^{(i)}\right)_{(n,q,k)} = \frac{\boldsymbol{I}_{n,q}^{\mathrm{CKT}}}{w} \int_{\partial\Omega_{i,port}} \boldsymbol{\Phi}_k^{(i)} \cdot \hat{\boldsymbol{l}}_q \mathrm{d}S = \boldsymbol{I}_{n,q}^{\mathrm{CKT}} \mathrm{G}_{q,k}^{(i)}. \tag{24}$$

The coupled local system equation can be established by combining (20), (23) and (24) and formulated as

$$\boldsymbol{F}(\boldsymbol{x}_{n+1}) = \boldsymbol{b}_n \tag{25}$$

where

$$\boldsymbol{x}_{n+1} = \begin{bmatrix} \boldsymbol{e}_{n+1}^{(i)} & \boldsymbol{V}_{n+1,q}^{\mathrm{CKT}} & \boldsymbol{I}_{n+1,q}^{\mathrm{CKT}} \end{bmatrix}^{\mathrm{T}} \tag{26}$$

$$\boldsymbol{F}(\boldsymbol{x}_{n+1}) = \begin{bmatrix} \left[\boldsymbol{M}_e^{(i)}\right] & \boldsymbol{0} & \Delta t \mathrm{G}_q^{(i)}/4 \\ \boldsymbol{0} & [Y]_q & -[B]_q \\ [C]_q^{(i)} & -[B]_q^{\mathrm{T}} & \boldsymbol{0} \end{bmatrix} \begin{bmatrix} \boldsymbol{e}_{n+1}^{(i)} \\ \boldsymbol{V}_{n+1,q}^{\mathrm{CKT}} \\ \boldsymbol{I}_{n+1,q}^{\mathrm{CKT}} \end{bmatrix} + \begin{bmatrix} \boldsymbol{0} \\ \boldsymbol{I}_{n+1,q}^{\mathrm{CKT,nl}} \\ -\boldsymbol{V}_{n+1}^{\mathrm{ind}} \end{bmatrix} \tag{27}$$

$$\boldsymbol{b}_n = \begin{bmatrix} \boldsymbol{b}_{\mathrm{EM}} \\ \boldsymbol{I}_{n,q}^{\mathrm{CP}} \\ \boldsymbol{0} \end{bmatrix} \tag{28}$$

with

$$\boldsymbol{b}_{\mathrm{EM}} = \boldsymbol{M}_e^{(i)} \boldsymbol{e}_n^{(i)} + \Delta t \left[\left(\boldsymbol{S}_e^{(i)} - \boldsymbol{F}_{eh}^{(ii)} \right) \boldsymbol{h}_{n+\frac{1}{2}}^{(i)} - \boldsymbol{I}_{n,q}^{\mathrm{CKT}} \mathrm{G}_q^{(i)} / 4 + \boldsymbol{F}_{eh}^{(ii)} \boldsymbol{h}_{n+\frac{1}{2}}^{(j)} \right]. \tag{29}$$

The overall dimension of the coupled system in (25) is equal to $n_e^{(i)} + N^{\mathrm{CKT}}$. Compared with the globally coupled FEM system, this system using DGFETD is very small. Note that the minus sign in front of the $[B]$ matrix is introduced since the current direction in our method is opposite to that defined in the standard MNA formulation. To tackle the instability issue caused by non-linear elements, the standard Newton-Raphson method is used with trivial computational cost due to the coupled small matrix system.

3 Numerical results

In this section, a parallel plate waveguide terminated by different lumped networks is employed to validate the proposed algorithm.

Figure 1: Geometrical structure of a parallel plate waveguide used to verify the proposed algorithm.

In the first example, a 1 cm waveguide is driven by a Thévenin voltage source as shown in Fig. 1 and terminated with a lumped network comprised of only linear lumped elements as shown in Fig. 2 is investigated. Two lumped ports are defined at the driven source and the load end of the waveguide, respectively. The Thévenin voltage source is a first order differential Guassian pulse. The amplitude and phase of the S parameter are presented in Fig. 3 and Fig. 4, respectively. The calculated input impedance is shown in Fig. 5. It can be explicitly noted that very good agreements are achieved from DC to 10 GHz.

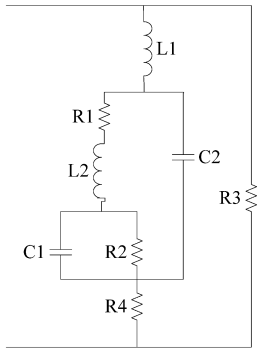

Figure 2: A single port lumped network containing only linear elements. The corresponding R, L, and C values are: $R_1 = 75\,\Omega$, $R_2 = 100\,\Omega$, $R_3 = 376.7\,\Omega$, $R_4 = 100\,\Omega$, $L_1 = 10\,\text{nH}$, $L_2 = 1\,\text{nH}$, $C_1 = 1\,\text{pF}$, $C_2 = 0.01\,\text{pF}$.

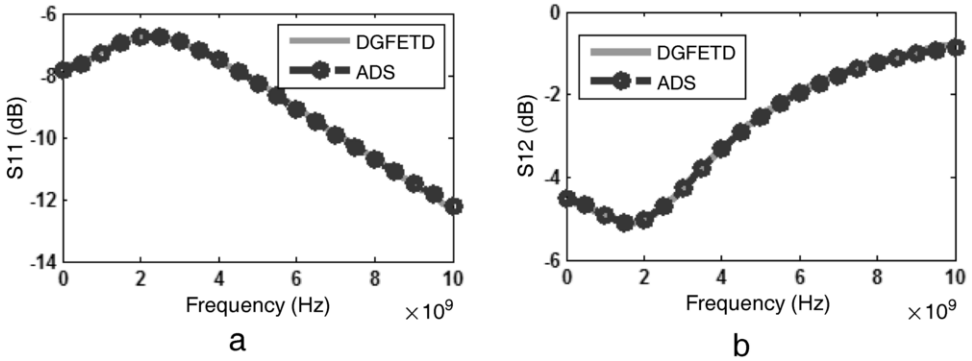

Figure 3: Magnitude of S_{11} and S_{21} calculated from the proposed hybrid EM-circuit simulator and ADS.

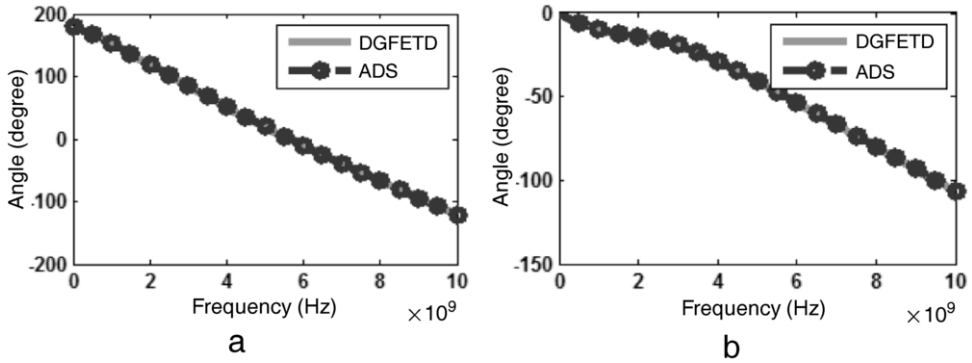

Figure 4: The phase of the S parameter. (a) Phase of S_{11}; (b) phase of S_{21}.

In the next example, the same parallel plate waveguide driven by a TEM wave is studied. It is loaded with silicon diodes ($i_D(t) = I_0[e^{V_D(t)/V_0} - 1], I_0 = 10^{-14}\,\text{A}, V_0 = 0.026\,\text{V}$) as shown in Fig. 5. Since this diode is a

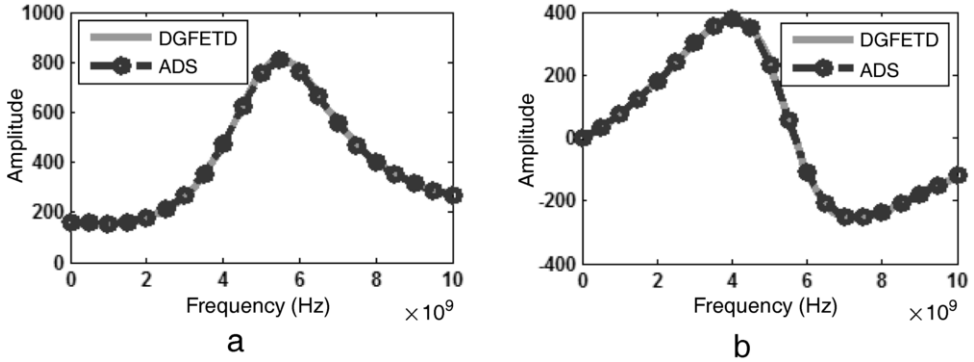

Figure 5: The real part (a) and the imaginary part (b) of the input impedance.

nonlinear device, the standard Newton-Raphson method is applied to handle the potential instability introduced by this non-linearity. The incident wave is a sinusoidal source oscillating at 2.5 GHz. The amplitude of this sinusoidal source is gradually increased, and the time domain voltage at the terminal of the diode in Fig. 6(a) is presented in Fig. 7(a) without any instability problem. It can be clearly noted that the maximum voltage at the diode terminal is around 0.7 V, which complies with the theory.

Finally, the diode pair in Fig. 6(b) is used to terminate the wave guide. This diode pair is capable of limiting the output voltage and is called the clamping diode. Theoretically, the output voltage should be clamped between -0.7 V and 0.7 V. To verify the validity of the proposed algorithm, the output voltage at this diode pair is shown in Fig. 7(b). The calculated result completely agrees with the theory.

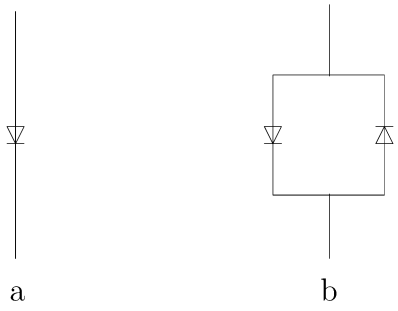

Figure 6: Diode and diode pair are used to validate the capability of the proposed algorithm to handle non-linear elements.

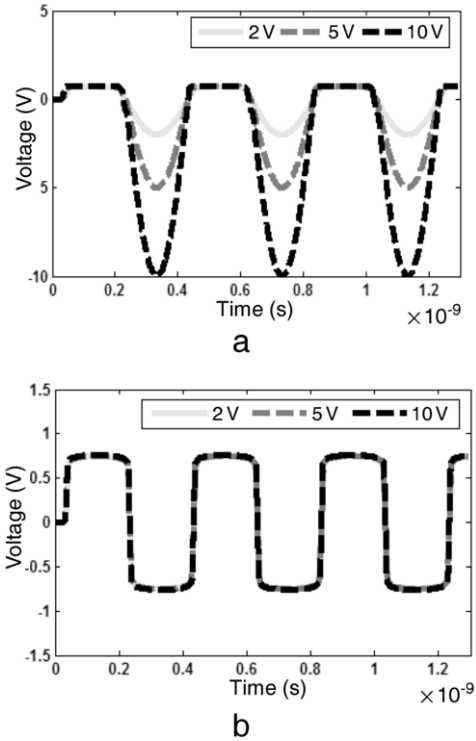

Figure 7: The time domain voltage at the terminal of the diode corresponding to excitations with different amplitude. (a) Output voltage of the diode in Fig. 6(a). (b) Output voltage of the clamping diode in Fig. 6(b).

4 Conclusion

In this work, a hybrid EM-circuit simulator based on the DGFETD and MNA is developed to model single port lumped networks. The interactions between the EM and circuit systems is achieved through a lumped port residing over a rectangular surface. Due to the local property of the DGFETD, the resultant coupled EM-circuit system is quite small. Thus, it can be solved with negligible cost even non-linear elements are included in the lumped network. To suppress the instability issue, the standard Newton-Raphson method is used to solve the non-linear system. The proposed algorithm is validated by numerical examples.

Ongoing work includes the modeling of multi-port lumped networks using DGFETD and MNA. These multi-port lumped networks contain either arbitrarily complex linear or non-linear devices such as power amplifiers, oscillators and so on.

Acknowledgment

The authors are grateful for the constructive suggestions from Professor Weng Cho Chew. We are also grateful to the supports from the Research Grants Council of Hong Kong (GRF 713011 and GRF 712612), National Science Foundation of China (NSFC 61271158), and in part by the University Grants Council of Hong Kong (Contract No. AoE/P-04/08).

Bibliography

[1] M. Piket-May, A. Taflove, and J. Baron, "FD-TD modeling of digital signal propagation in 3-D circuits with passive and active loads," *IEEE Trans. Microw. Theory Tech.*, vol. 42, no. 8, pp. 1514–1523, Aug. 1994.

[2] C. N. Kuo, R. B. Wu, B. Houshmand, and T. Itoh, "Modeling of microwave active devices using the FDTD analysis based on the voltage-source approach," *IEEE Microwave Guided Wave Lett.*, vol. 6, pp. 199–201, Apr. 1996.

[3] C. C. Wang and C. W. Kuo, "An efficient scheme for processing arbitrary lumped multiport devices in the finite-difference time-domain method," *IEEE Trans. Microw. Theory Tech.*, vol. 55, no. 5, pp. 958–965, May 2007.

[4] R. Wang and J. M. Jin, "A symmetric electromagnetic-circuit simulator based on the extended time-domain finite element method," *IEEE Trans. Microw. Theory Tech.*, vol. 56, no. 12, pp. 2875–2884, Dec. 2008.

[5] R. Wang and J. M. Jin, "Incorporation of multiport lumped networks into the hybrid time-domain finite-element analysis," *IEEE Trans. Microw. Theory Tech.*, vol. 57, no. 8, pp. 2030–2037, Aug. 2009.

[6] Q. He and D. Jiao, "Fast electromagnetic-based co-simulation of linear network and nonlinear circuits for the analysis of high-speed integrated circuits," *IEEE Trans. Microw. Theory Tech.*, vol. 58, no. 12, pp. 3677–3687, Dec. 2010.

[7] S. D. Gedney, C. Luo, J. A. Roden, R. D. Crawford, B. Guernsey, J. A. Miller, T. Kramer, and E. W. Lucas, "The discontinuous Galerkin finite-element time-domain method solution of Maxwell's equations," *Journal of Applied Comput. Electromag. Society* , vol. 24, no. 2, pp. 129–142, Apr. 2009.

[8] S. Dosopoulos and J. F. Lee, "Interconnect and lumped elements modeling in interior penalty discontinuous Galerkin time-domain methods," *J. Comput. Phys.*, vol. 229, no. 22, pp. 8521–8536, Nov. 2010.

[9] B. Zhao, J. C. Yong, and S. D. Gedney, "SPICE lumped circuit subcell model for the discontinuous Galerkin finite element time-domain method," in *Proc. IEEE Int. Symp. on Antennas Propag.*, pp. 2969-2971, Spokane, WA, July 2011.